Al doping influence on crystal growth, structure and superconducting properties of Y(Ca)Ba2Cu3O7y whiskers

Al doping influence on crystal growth, structure and superconducting properties of $Y(Ca)Ba_2Cu_3O_{7-y}$ whiskers

L. Calore[a], M.M. Rahman Khan[a,b], S. Cagliero[a,*], A. Agostino[a], M. Truccato[c], L. Operti[a]

[a] *NIS-Centre of Excellence, Department of Chemistry, University of Torino, Via P. Giuria 7, I-10125 Torino, Italy*

[b] *Department of Chemistry, Shahjalal University of Science and Technology, Sylhet 3114, Bangladesh*

[c] *CNISM and NIS Center of Excellence, Department of Physics, University of Torino, Via P. Giuria 1, I-10125 Torino, Italy*

* Corresponding author. *E-mail address:* stefano.cagliero@unito.it

Abstract

We synthesized Al doped $Y(Ca)Ba_2Cu_3O_{7-y}$ (YBCO) whiskers via the solid state reaction method. Al doping was systematically varied in the nominal cationic stoichiometry of $YBa_2Cu_3CaTe_{0.5}Al_xO_{7-y}$, with $0 \leq x \leq 0.5$. The amount of the grown whiskers increases for nominal Al addition up to $x = 0.05$, decreasing for larger concentrations. The concentration of Al incorporated in the crystals (x') is always higher with respect to the starting stoichiometry and shows a gradient along its length, with a higher amount

at the tip regions. The single crystal diffraction analyses show an increasing tetragonal character with increasing x', with a transition from the orthorhombic to the tetragonal system for $x' = 0.13$, which is in agreement with the worsening of electrical transport properties and disappearing of superconductivity for $x' = 0.19$.

Keywords: Oxide superconductors Whiskers Superconductivity Powders-solid state reaction Growth mechanism

1. Introduction

Stacks of Intrinsic Josephson Junctions (IJJs) with atomic size are naturally formed in layered high-T_C superconductors (HTS) such as $Bi_2Sr_2CaCu_2O_{8+d}$ (Bi-2212), $La_{2-x}Sr_xCuO_4$ (LSCO) and RE-123 (Rare Earth = Y, Eu, Gd, Dy, Ho, Er, Tm, and Lu) [1–4]. IJJs have been pro- posed as modular elements in the realization of various cryogenic devices, such as THz emitters/sensors [5], micro-SQUIDs' [6], and quantum bit-computing based on Macroscopic Quantum Tunneling phenomena [7].

Among the possible IJJs applications, high frequency devices can take advantage from the large Josephson plasma frequency found in some HTS. For instance, Y-123 has a Josephson plasma frequency close to a few THz because of its low anisotropy and high critical current densities [8], which makes it a suitable candidate for the fabrication of these devices. Furthermore, such properties could be modulated by cationic substitutions as already noticed for Pb doped Bi-2212 [9].

In a future context of IJJs exploitation, HTS whiskers, like the ones belonging to the YBCO system, are suitable for studies and devices based on IJJs, which require high homogeneity of IJJs proper- ties on the micrometric scale. Their highly crystalline nature, low defect concentration and excellent superconducting features pro- vide this aspect. Moreover, starting from a micrometric cross section, they are easily scalable by etching techniques down to sub-micrometric sizes and are also very suitable for 3D machining, resulting in solid-state devices with a high degree of miniaturization [3,4,10].

One of the main concerns about YBCO whiskers employment for these kinds of investigation is their synthesis in useful quantities, with respect to the BSCCO counterpart. As a matter of fact, much information is given in the literature about BSCCO whiskers and what is favoring or allowing their growth [11]. In this case, alumina addition as a precursor dopant has been found to drastically enhance the formation of such whiskers [12–15]. Moreover, Al together with Te represents the most efficient combination to favor the growth of Bi-2212 whiskers [12].

About YBCO whiskers the present situation is quite different. Although the growth of pure Y-123 whiskers has already been shown [16], the fact that Ca-doping of Y-123 can increase the carrier density in underdoped material [17] and also enhance both the values and the isotropy of the critical current density, J_C [18,19] makes Ca-doped YBCO

whiskers interesting. Indeed, also this kind of whiskers has been synthesized by Nagao et al. making combined use of Ca- and Te-based precursors [20]. However, in spite of the dramatic effect that alumina has on the growth of BSCCO whiskers, no corresponding investigation has been carried out so far about its influence in promoting the Y-123 whisker growth, neither in the pure nor in the Ca-doped form.

Concerning the influence of Al doping on the structure and superconducting properties of Y-123, this topic has been studied by many authors both in polycrystalline samples and in bulk single crystals. For instance, Al was incorporated from alumina crucibles used during the synthesis process or from Al_2O_3 nanoparticle addition in Y-123 ceramics, showing a substantial effect on the structure as well as the worsening of the superconducting properties in both cases [21–23]. About these general aspects, a systematic study of Al doping in Y-123 whiskers could extend the knowledge by giving more precise indications thanks to their microcrystalline nature and low defectivity.

It is therefore expected that the addition of alumina in the growth process of Y-123 whiskers on one hand could favor the growth of the crystals but on the other hand could also introduce detrimental effects in their superconducting properties that partially or fully counteract the beneficial effects of Ca addition. To the best of our knowledge, no information is available about this issue and new experiments on the growth of simultaneously Al- and Ca-doped whiskers are needed to clarify the interplay of these two elements and possibly to identify the best compromise in terms of both crystal yield and material properties. The present work is intended to provide such information by performing a systematic study of alumina addition in the growth of Ca-doped Y-123 whiskers and checking its effects in terms of growth process, crystal structure and superconducting properties.

2. Experimental details

Powders with nominal cationic composition of $YBa_2Cu_3CaTe_{0.5}Al_x$ were prepared according to the previously reported procedure by the solid state reaction of individual component Y_2O_3(99.99%), $BaCO_3$(99.999%), CuO(99.9999%), $CaCO_3$(99.9999%), TeO_2(99.995%) and Al_2O_3(99.998%) (Sigma–Aldrich, Germany) [20]. The nominal amounts of Al in the precursor pellets used for different synthesis batches were x = 0, 0.025,

0.050, 0.075, 0.100, 0.250 and 0.500. The precursor powders were thoroughly mixed and calcined at 900 °C in alumina crucibles for 10 h in air with three intermediate grindings. The calcined powders were then pressed into pellets of about 13 mm in diameter and 2 mm in thickness, which were subsequently put in a pure alumina boat and placed in a tube furnace of 150 cm in length and 4 cm in internal diameter. For the thermal treatment we used a controlled oxy- gen flow (0.2 l/min) and a thermal cycle of T_{max} = 1005 °C, t_{max} = 5 h and T_e = 925 °C for all the synthesis sets, where T_{max} is the maximum temperature set in the increasing ramp, t_{max} is the dwell time at T_{max} and T_e is the thermal treatment end point temperature, at which the oven was turned off for furnace cooling. All the syntheses were performed following constant heating and cooling ramps at 5 °C/min and 1 °C/h, respectively.

SEM (Scanning Electron Microscope) and EDS (Energy Dispersive Spectrometer) measurements were performed with a Leica Steroscan 420 equipped with the INCA Oxford software on all of the seven synthesis batches in order to obtain information on surface morphologies and cationic stoichiometries.

Crystallographic data were collected at a Gemini R Ultra single crystal diffractometer operating at 50 kV and 40 mA, with a graphite-monochromatized Mo Ka radiation source and by using an ω-scan technique (Dω = 1.0°). CrysAlis PRO software has been used for data collection and reduction (peak intensity integration, background evaluation, cell parameters and space group determination) [24].

In order to prepare the samples for electrical characterization, we selected, by optical microscope observation, very regular YBCO whiskers from each of the synthesized batches. Four silver contacts were fabricated on each crystal by physical vapor deposition through a steel mask. Resistance versus temperature data were acquired by means of a standard four-probe technique in the range of 77.6–300 K at the constant rate of 0.2 K/min and feeding the crystals with current pulses in the 1– 5 μA range. Resistivity curves were calculated after accurate measurements of the sample geometry by means of SEM and AFM (Atomic Force Microscopy) characterizations and T_c values were evaluated as the midpoint of the resistivity curves. For electrically measured samples EDS analyses were performed between the voltage contacts (i.e. in the sensed region), while for samples used for single crystal diffraction such analyses were performed along the crystal length to evaluate the concentration of Al at different spots of the crystals.

3. Results and discussion

3.1. *SEM and EDS analysis*

Fig. 1 shows two SEM micrographs representing the $YBa_2Cu_3CaTe_{0.5}Al_x$ synthesis batches with $x = 0$ (Fig. 1a) and $x = 0.050$ (Fig. 1b). It is possible to notice that for $x = 0$ fewer whiskers are visible with respect to the $x = 0.050$ batch.

Indeed, we observed an increase in the amount of whiskers with increasing the Al content, up to a maximum for $x = 0.050$. Then the whisker amount decreased for higher Al_2O_3 contents. Similar effects have already been observed on the growth of Bi-2212 whiskers and are associated to the release of an appropriate amount of Al^{3+} ions in the pellet, playing an important role in nucleation [13,15].

Table 1 lists typical atomic ratios resulting from EDS analysis of the different growth batches. It is worth mentioning that it was not possible to disentangle the *T*e contribution due to the overlapping of the corresponding peak with the *K*a line of Ca. Therefore the *T*e content resulted below the detection limit in all cases and could not be reported. It is possible to observe from Table 1 that the amount of Al ions that really enters the crystals (labeled as *x'*) in- creases with increasing the nominal Al content of the batch (labeled as *x*).

In more detail, it can be noticed that for the Al-free whiskers ($x = 0$) the normalized atomic ratios Y:Ca:Ba:Cu = 1:0.11:1.94:2.5 are very similar to those reported for Y(Ca)-123 whiskers in previous works [20,25]. Moreover, in the case of $x = 0.025$ the deter-mined ratios of Y:Ca:Ba:Cu:Al = 1:0.14:2.20:2.98:0.084 are analogous to the ones reported in the literature for Ca-doped Y- 123 whiskers [20] and Al-doped Y-123 single crystals [22]. It is important to observe that in the former case the samples were not prepared using Al doping, while in the latter case the authors did not use Ca in the material synthesis. Nevertheless, our results show that both of these elements can be simultaneously incorporated in YBCO whiskers.

SEM observations showed that alumina addition not only affect the whisker amount and the chemical composition of the crystals, but also their surface morphology. Fig. 2 shows three SEM micrographs obtained for the $x = 0.025$ batch (Fig. 2a), $x = 0.050$ (Fig. 2b)

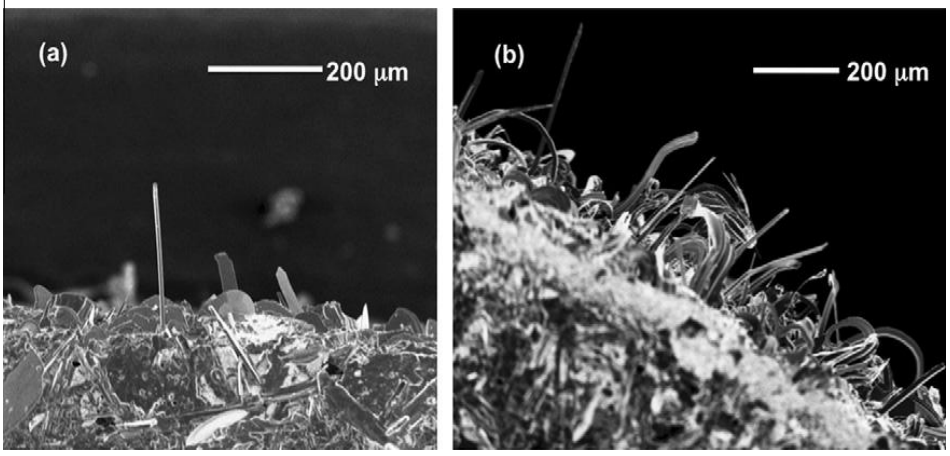

Fig. 1. SEM images of Y(Ca)Ba2Cu3Al*x*O7—*y* crystals obtained from two different synthesis batches. (a) corresponds to the $x = 0$ batch and (b) corresponds to the $x = 0.050$ batch.

x	Ca	Ba	Cu	Al(x')
0	0.11	1.94	2.5	0
0.025	0.14	2.20	2.98	0.084
0.050	0.13	2.26	2.79	0.13
0.075	0.13	2.13	3.07	0.19
0.100	0.14	2.04	2.94	0.38
0.500	0.18	2.00	3.30	2.54

Table 1: Typical atomic ratios resulting from EDS analysis for whiskers grown from the YBa2Cu3CaTe0.5Al*x* synthesis batches. All results are normalized to $Y = 1$. Al amount really incorporated into the crystals has also been labeled as x'.

and $x = 0.500$ (Fig. 2c). In Fig. 2a, a thin Al-doped (Y,Ca)-123 whisker is clearly visible at the center of the image (marked by a white cross). Such crystal, as most of the whiskers observed in the same batch, has a very smooth surface and a sharp profile (a smaller crystal with the same characteristics is also visible on its left). Concerning Fig. 2b ($x = 0.050$), a smooth surface can still be observed for this crystal, as in the case of the other batches with a low aluminum content ($x = 0.025$–0.050). Increasing aluminum in the nominal stoichiometric ratio (especially in the range $x = 0.100$–0.500) the crystals become rough and irregular: an example of this kind of whiskers can be seen in Fig. 2c, where a crystal obtained from the synthesis batch $x = 0.500$ is shown. Such morphological trend is thus clearly correlated to the amount of Al incorporated in the sample, as it is apparent from the values of x' listed in Table 1.

In order to clarify the relationship between the nominal and incorporated Al

concentrations, we performed a series of EDS measurements on several whiskers selected from batches x = 0.025, 0.050 and 0.075, also taking into consideration possible Al variations along the crystal length. In particular, we have measured the Al content at the base, middle and tip regions on five whiskers selected for each of the mentioned batches (15 crystals in total), then we have calculated the average and standard deviation values of Al concentration in each region. Fig. 3 shows these values as a function of the whisker region and of the synthesis batch: red circles (dashed line) represent the x = 0.025 batch, black squares (solid line) represent the x = 0.050 batch, green triangles (dotted line) represent the x = 0.075 batch.

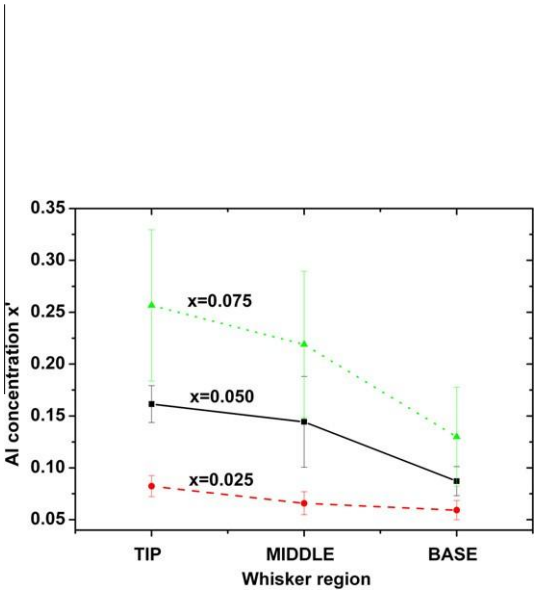

Fig. 3. Al concentration versus whisker regions. Red circles, black squares and green triangles represent synthesis x = 0.025, 0.050 and 0.075, respectively. Connection lines are guides for the eye. (For interpretation of the references to color in this figure legend, the reader is referred to the web version of this article.)

From Fig. 3, several observations can be inferred: (i) the mean Al value incorporated in the crystal is always higher than the nominal amount of the synthesis, (ii) the difference between nominal and really incorporated concentrations increases on the average with increasing the nominal Al content, (iii) there is an average concentration gradient along the crystal length, with higher Al concentrations corresponding to the tip regions, which becomes more evident with increasing the nominal Al amount, (iv) the standard deviations (reported as error bars in Fig. 3) increase with the nominal Al amount: the

fluctuations of Al incorporation in different whiskers from the same pellet increase for higher nominal Al values. Concerning the latter consideration, since the Al_2O_3 distribution in the precursor pellets is not homogenous, the growth of whiskers with different Al content depends on the starting local composition of the precursor. This observation well correlates with the one of the increased number of crystals present in synthesis batches with higher nominal Al content, supporting the picture of a very active role of Al in the synthesis because of the induction of heterogeneous nucleation. Concerning this growth process, the gradient of Al concentration found along the whisker length suggests that a micro-crucible model can be applied to the crystal development with a bottom-up mechanism. Such kind of development has been already proposed by many authors for Bi-2212 whiskers, but its validity is still under discussion since several other options have also been proposed [12]. In our case, the bottom-up mechanism seems to be confirmed, since, being linked with a local micro-crucible, it would imply the reduction of Al amount at the whisker growing site during the growth process, being maximum at the initial phases of the whisker formation (tip region) and decreasing at the following stages (middle and base regions). It is also worth pointing out that such results perfectly fit into the size changing, moving and multiple growth inter- face (SCMMGI) model recently developed to explain the growth of curved whiskers both of the BSCCO and of the YBCO systems [26]. Since, based on the previous observations, the Al amount incorporated in the crystals is always higher with respect to the nominal one, in the following structural and electrical studies we will refer to the real Al amount x', as obtained in each case by EDS measurements.

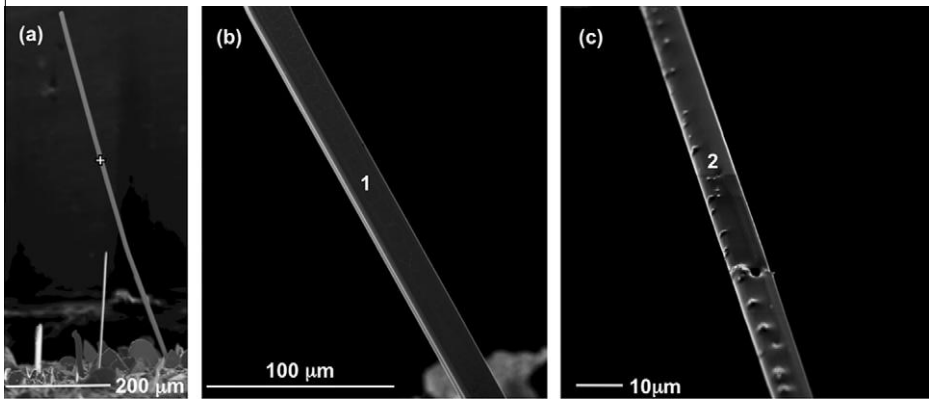

Fig. 2. SEM micrographs of Al-doped (Y,Ca)-123 crystals synthesized with different alumina addition. (a) corresponds to batch $x = 0.025$, (b) represents batch $x = 0.050$, (c) obtained from batch $x = 0.500$. The white cross marker, numbers 1 and 2 indicate the points where EDS analyses were performed.

3.2. *Single crystal X-ray diffraction*

In order to obtain information on the structure of whiskers with different amounts of Al, we have collected several crystals from different batches with increasing nominal Al composition. Among them we have selected four whiskers with increasing Al content x', evaluated as the average value of Al content at the tip, middle and base regions by EDS analysis. These samples have then been measured by single crystal diffraction. To evaluate the single crystal quality of the whiskers, each of them underwent a preliminary analysis by recording its full rotation photograph, which confirmed the presence of a single individual. More details on the acquisition of the complete data sets, like for instance the number of reflections that have been collected and indexed, are reported in Table 2.

This table also lists the structural parameters obtained for the selected whiskers, corresponding to $x' = 0$, 0.084, 0.13 and 0.38. The Al-free sample presents an orthorhombic cell with parameter values in good agreement with the bulk Y-123 material obtained with a flowing oxygen treatment, similar to our synthesis process [21]. It is not possible to compare these values with previous cell evaluations on YBCO whiskers since, to the best of our knowledge, they have not been reported before.

Moreover, Table 2 shows that for the samples with a higher Al content ($x' = 0.084 – 0.38$) the crystalline system is less orthorhombic, switching to the tetragonal phase at $x' = 0.13$. The observed behavior is in agreement with previous data obtained on bulk crystals and polycrystalline samples [21,22,27]. In such papers the cell modifications are correlated with the substitution of Al on the Cu(1) sites, along the Cu–O chains. Indeed, since Al is more stable in an octahedral oxygen coordination, which is possible only if oxygen is added to all of the adjacent sites, the increase in Al con- tent induces an increase in the cross-linking of Cu–O chains and therefore a more tetragonal symmetry of the crystals [22]. Concerning the *c*-axis parameter, shorter values were observed for the tetragonal phase, in accordance with the cited publications, as a consequence of the shorter Al–O distance compared to the Cu–O distance along the *c*-axis.

3.3. *Electrical characterization*

The four-probe electrical transport measurements of five crystals selected from different batches are shown in Fig. 4, reporting the q_{ab} versus T data. For all the crystals we also evaluated the Al concentration by EDS analysis, being aware of the difference between the nominal amount and the really incorporated value. Therefore, we obtained specific Al concentrations to be correlated with the electrical characteristics, as reported in Fig. 4 for each resistivity curve. It can be noticed that the sample with $x' = 0.100$ (red dashed curve) shows a higher resistivity compared to the zero Al-doped sample (black dotted curve). Even higher resistivity val- ues are observed for the $x' = 0.150$ sample (green dash-dotted curve). The sample with Al incorporated amount $x' = 0.19$ shows a semiconducting-like behavior with no superconducting transi- tion down to 77 K (blue dashed-dotted curve). Finally, the whisker with an incorporated Al amount of $x' = 0.62$ presents a practically temperature-independent resistivity behavior with no superconducting transition, resembling that of insulating materials. How- ever, a crossover is present between the curves corresponding to $x' = 0.19$ and $x' = 0.62$ around $T = 190$ K.

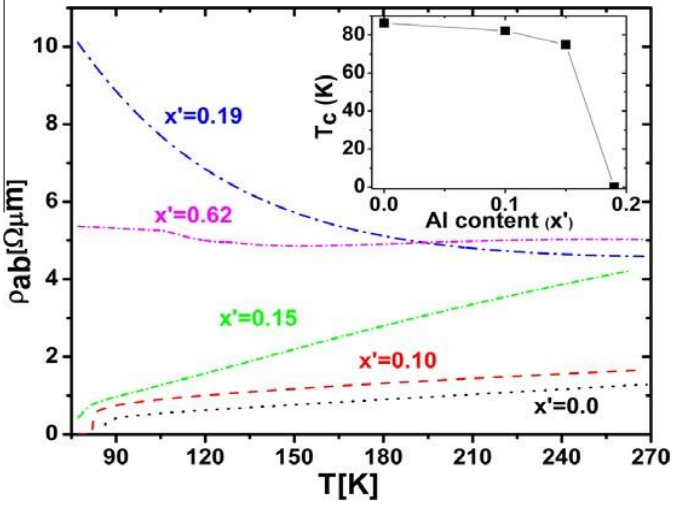

Fig. 4. Temperature dependence of the in-plane resistivity q_{ab} of (Y,Ca)-123 whiskers with increasing Al content. The inset reports the T_C values versus Al content x' ($x' = 0.62$ is not reported for graphical reasons).

The Al content affects not only the resistivity behavior of the whiskers, but also their T_C values, which are reported in the inset of Fig. 4. The Al-free sample shows a T_C value of 86.3

K, while for the x' = 0.1 sample we observed a T_C = 82.2 K. Finally, for the x' = 0.15 sample the transition is not concluded at 77.7 K, but from the slope of the starting part of the transition we have extrapolated a value of T_C = 75 K. Based on these results, there is an evident T_C decrease with increasing the alumina amount x'.

All of these observations are in agreement with previous works on Al doping in bulk crystals, where low concentrations of Al bring a decrease of T_C and the switch from superconducting to insulating behavior takes place for Al concentration of about x = 0.2 [21,22,28]. The gradual suppression of superconductivity is usually associated with the variation of the oxygen content supported by the increased Al concentration and the overlapping of disordered regions [21,22]. In this framework, our observation of a temperature-independent resistivity behavior for x' = 0.62 seems to indicate that, at so high Al concentrations, the disorder induced by the random presence of Al atoms in the lattice becomes the most limiting factor for the electrical conductivity.

Aluminum content	x' = 0	x' = 0.084	x' = 0.13	x' = 0.38
No. of reflections	1081	1667	1907	3659
No. of unique reflections	234	353	286	233
a (Å)	3.8176(2)	3.8380(2)	3.8404(3)	3.8592(2)
b (Å)	3.8736(2)	3.8728(2)	3.8404(3)	3.8592(2)
c (Å)	11.6793(4)	11.6914(5)	11.604(1)	11.6437(8)
Crystalline system	Orthorhombic	Orthorhombic	Tetragonal	Tetragonal
Space group	Pmmm	Pmmm	P4/mmm	P4/mmm

Table 2: Details of single crystal X-ray data acquisition and corresponding cell parameters for four whiskers with different aluminum concentration x'. All angles of the unit cell are 90°.

4. Conclusions

The Al addition in YBCO whiskers was systematically varied in the nominal stoichiometry of $YBa_2Cu_3CaTe_{0.5}Al_x$ with $0 \leq x \leq 0,5$. It has been observed that moderate additions of alumina in the precursor pellet increase the amount of whiskers, due to the in- crease of nucleation sites. This result, together with the Al concentration gradient found along the whisker length, represents a new evidence for the bottom-up growth mechanism, already discussed for Bi-2212 whiskers. Moreover, we have noticed that the real value of Al incorporated in the crystal is always higher with respect to the

nominal amount of the precursor pellet, testifying an active role of Al in the growth.

Structural and electronic properties have been noticed to change as a function of the Al content: a gradual decrease of the whisker T_c at low Al concentrations is related to the crystal structure modification with converging *a* and *b* lattice parameters. The crystals switch to the tetragonal phase for average Al contents of $x' = 0.13$ and become non-superconducting for values of $x' = 0.19$.

Summarizing, we can state that a maximum nominal Al addition in the range of $x = 0.025–0.05$ is advisable for the synthesis of YBCO whiskers in order to increase the amount of grown crystals while preserving good superconducting properties. We think that such conclusions offer new perspectives on the YBCO whisker synthesis as a valid alternative to bulk single crystals, which require more complex and expensive equipment, and represent an useful starting point for future work on IJJs properties modulation.

Acknowledgments

We acknowledge financial support by the project ORTO11RRT5 in the framework of Progetti di Ricerca di Ateneo–Compagnia di San Paolo–2011.

References

[1] R. Kleiner, F. Steinmeyer, G. Kunkel, P. Muller, Phys. Rev. Lett. 68 (1992) 2394–2397.

[2] Y. Kubo, T. Tanaka, Y. Takahide, S. Ueda, T. Okutsu, A.T.M.N. Islam, I. Tanaka, Y. Takano, Physica C 468 (2008) 1922–1924.

[3] T. Okutsu, S. Ueda, S. Ishii, M. Nagasawa, Y. Takano, Physica C 468 (2008) 1929–1931.

[4] T. Kawae, M. Nagao, Y. Takano, H.B. Wang, T. Hatano, T. Yamashita, Physica C 426 (2005) 1479–1483.

[5] L. Ozyuzer, A.E. Koshelev, C. Kurter, N. Gopalsami, Q. Li, M. Tachiki, K. Kadowaki, T. Yamamoto, H. Minami, H. Yamaguchi, T. Tachiki, K.E. Gray, W.K. Kwok, U. Welp, Science 318 (2007) 1291–1293.

[6] M. Sandberg, V.M. Krasnov, Phys. Rev. B 72 (2005) 212501.

[7] K. Inomata, S. Sato, K. Nakajima, A. Tanaka, Y. Takano, H.B. Wang, M. Nagao, H. Hatano, S. Kawabata, Phys. Rev. Lett. 95 (2005) 107005.

[8] H. Shibata, T. Yamada, Physica C 293 (1997) 191–195.

[9] H. Kambara, I. Kakeya, M. Suzuki, Physica C 471 (2011) 754–757.

[10] K. Inomata, T. Kawae, S.J. Kim, K. Nakajima, T. Yamashita, M. Nagao, H. Madea, Physica C 372 (2002) 335–338.

[11] T.E. Oskina, Y.G. Ponomarev, H. Piel, Y.D. Tretyakov, B. Lehndorff, Physica C 266 (1996) 115–126.

[12] P. Badica, K. Togano, S. Awaji, K. Watanabe, H. Kumakura, Supercond. Sci. Technol. 19 (2006) R81–R99.

[13] I. Matsubara, R. Funahashi, T. Ogura, H. Yamashita, K. Tsuru, T. Kawai, J. Cryst. Growth 141 (1994) 131–140.

[14] T. Kasuga, H. Kimura, Y. Ishigure, Y. Abe, J. Cryst. Growth 144 (1994) 375–379.

[15] Y. Abe, K. Hirata, H. Hosono, Y. Kubo, J. Mater. Res. 7 (1992) 1599–1601.

[16] M. Nagao, T. Kawae, K. Yun, H.B. Wang, Y. Takano, T. Hatano, T. Yamashita, M. Tachiki, H. Maeda, M. Sato, J. Appl. Phys. 98 (2005) 073903.

[17] V.P.S. Awana, A. Tulapurkar, S.K. Malik, A.V. Narlikar, Phys. Rev. B 50 (1994) 594–596.

[18] G. Hammerl, A. Schmehl, R.R. Schulz, B. Goetz, H. Bielefeldt, C.W. Schneider, H. Hilgenkamp, J. Mannhart, Nature 407 (2000) 162–164.

[19] N.A. Rutter, J.H. Durrell, M.G. Blamire, J.L. McManus-Driscoll JL, H. Wang, S.R. Foltyn, Appl. Phys. Lett. 87 (2005) 162507.

[20] M. Nagao, M. Sato, H. Maeda, K.S. Yun, Y. Takano, T. Hatano, S. Kim, Appl. Phys.Lett. 82 (2003) 1899–1901.

[21] V. Antal, K. Zmorayova, J. Kovac, V. Kavecansky, P. Diko, M. Eisterer, H.W. Weber, Supercond. Sci. Technol. 23 (2010) 065014.

[22] T. Siegrist, L.F. Schneemeyer, J.V. Waszczak, N.P. Singh, R.L. Opila, B. Batlogg, L.W. Rupp, D.W. Murphy, Phys. Rev. B 36 (1987) 8365–8368.

[23] J.P. Franck, J. Jung, M.A.K. Mohamed, Phys. Rev. B 36 (1987) 2308–2310.

[24] Agilent Technologies UK Ltd., UK, CrysAlisPro Software system, Version 1.171.35.19, 2012.

[25] R. Giri, V.P.S. Awana, H.K. Singh, R.S. Tiwari, O.N. Srivastava, A. Gupta, B.V. Kumaraswamy, H. Kishan, Physica C 419 (2005) 101–108.
[26] P. Badica, A. Agostino, M.M. Rahman Khan, S. Cagliero, C. Plapcianu, L. Pastero, M. Truccato, Y. Hayasaka, G. Jakob, Supercond. Sci. Technol. 25 (2012) 105003.
[27] J.M. Tarascon, P. Barboux, P.F. Miceli, L.H. Greene, G.W. Hull, M. Eibschutz, S.A. Sunshine, Phys. Rev. B 37 (1988) 7458–7469.
[28] Y.F. Zhang, D.D. Wang, P.L. Li, Low Temp. Phys. 36 (2010) 162–166.